



## Experiment Report Form

**The double page inside this form is to be filled in by all users or groups of users who have had access to beam time for measurements at the ESRF.**

Once completed, the report should be submitted electronically to the User Office via the User Portal:

<https://www.esrf.fr/misapps/SMISWebClient/protected/welcome.do>

### ***Reports supporting requests for additional beam time***

Reports can be submitted independently of new proposals – it is necessary simply to indicate the number of the report(s) supporting a new proposal on the proposal form.

The Review Committees reserve the right to reject new proposals from groups who have not reported on the use of beam time allocated previously.

### ***Reports on experiments relating to long term projects***

Proposers awarded beam time for a long term project are required to submit an interim report at the end of each year, irrespective of the number of shifts of beam time they have used.

### ***Published papers***

All users must give proper credit to ESRF staff members and proper mention to ESRF facilities which were essential for the results described in any ensuing publication. Further, they are obliged to send to the Joint ESRF/ ILL library the complete reference and the abstract of all papers appearing in print, and resulting from the use of the ESRF.

Should you wish to make more general comments on the experiment, please note them on the User Evaluation Form, and send both the Report and the Evaluation Form to the User Office.

### **Deadlines for submission of Experimental Reports**

- 1st March for experiments carried out up until June of the previous year;
- 1st September for experiments carried out up until January of the same year.

### **Instructions for preparing your Report**

- fill in a separate form for each project or series of measurements.
- type your report, in English.
- include the reference number of the proposal to which the report refers.
- make sure that the text, tables and figures fit into the space available.
- if your work is published or is in press, you may prefer to paste in the abstract, and add full reference details. If the abstract is in a language other than English, please include an English translation.



**Experiment title:** Deciphering the mechanism by which incorporated amino acids increase the band gap of their inorganic semiconductor hosts.

**Experiment number:**  
MA-2916

**Beamline:**

**Date of experiment:**

from: 8.06.2016 to: 14.06.2016

**Date of report:**

20.09.2016

**Shifts:**

**Local contact(s):**

Catherine Dejoie

*Received at ESRF:*

**Names and affiliations of applicants** (\* indicates experimentalists):

Department of Materials Science and Engineering and the Russel Berrie Nanotechnology Institute, Technion-Israel Institute of Technology, 32000 Haifa, Israel:

1. Boaz Pokroy
2. Iryna Polishchuk
3. Eva Weber

## Report:

During our experiment at ESRF beam ID22, we measured XRD diffractions of  $\text{Cu}_2\text{O}$  and  $\text{ZnO}$  powders modified with different biologically originated molecules. Specific biomolecules (amino acids) and peptides in various concentrations were added during the crystallization process in order to examine their effect on the micro and nano structure of the semiconducting crystals. Our goal was to determine lattice parameters changes via measuring the diffraction peak positions and utilizing Rietveld analysis method. Furthermore, our goal was to prove that incorporation of different biomolecules within the crystal structure of a semiconductor can be used for a technological application such as band gap engineering.

Analysing the data we collected during our stay at the ID22 we found that biomolecules incorporated into  $\text{Cu}_2\text{O}$  structure similar to  $\text{ZnO}$ , indeed, have a strong effect on the lattice parameters caused by intracrystalline strain. This result can be seen from Figure 1, presenting the most intense (111) peak ( $\theta = 11.55^\circ$ ) of different  $\text{Cu}_2\text{O}$  samples grown in the presence of various biomolecules. A clear shift of the diffraction peak position can be noticed for all investigated samples. Moreover, it can be seen from the Figure 1 that diffraction peaks returned to the original position (indicated by pure  $\text{Cu}_2\text{O}$  sample) after a mild heat treatment at  $250^\circ\text{C}$  due to strain release caused by amino acid destruction. Interestingly, in case of  $\text{Cu}_2\text{O}$ /amino acids composite crystals we observed a considerable shift towards higher  $2\theta$  indicating decrease in the lattice parameters upon incorporation of the amino acids into the  $\text{Cu}_2\text{O}$  crystal structure. In

contrast to the previously observed lattice expansion caused by intracrystalline such a negative lattice distortions upon incorporation we observed for the first time.

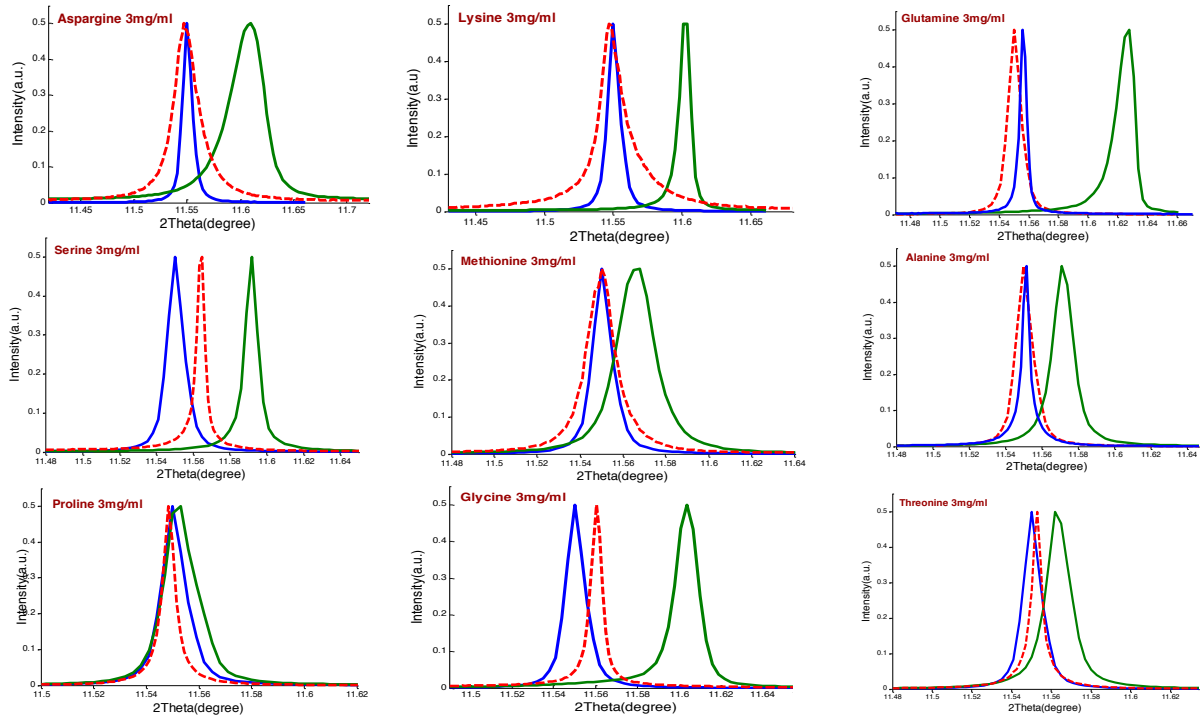


Figure 1. The (111) diffraction peak of the  $\text{Cu}_2\text{O}$  crystals grown in the presence of various biomolecules. The diffraction peak shift towards higher 2theta position indicates a shrinkage of the lattice parameters for composite crystals.

Utilizing Rietveld method we extracted lattice parameters for all the investigated samples and calculated corresponding lattice distortions for every sample. Table1 summarize these results.

Table 1. Rietveld analysis results.

Sample	AA concentration, $\text{mg/ml}^{-1}$	Lattice parameter, $\text{\AA}$	Lattice distortions	Goodness of fit parameter, $\chi^2$
$\text{Cu}_2\text{O}$ -Ref	-	4.269749		3.238
$\text{Cu}_2\text{O}$ -Ref-Heated	-	4.270063	2.06E-04	6.887
$\text{Cu}_2\text{O}$ -Asn3	3	4.246610	-5.42E-03	3.566
$\text{Cu}_2\text{O}$ -Asn3-Heated	3	4.269947	4.64E-05	2.36
$\text{Cu}_2\text{O}$ -Gln3	3	4.239428	-7.10E-03	2.851
$\text{Cu}_2\text{O}$ -Gln3-Heated	3	4.269142	-1.42E-04	8.653
$\text{Cu}_2\text{O}$ -Gly3	3	4.249225	-4.81E-03	2.509
$\text{Cu}_2\text{O}$ -Gly3-Heated	3	4.265816	-9.21E-04	4.386
$\text{Cu}_2\text{O}$ -Met3	3	4.262700	-1.65E-03	1.603
$\text{Cu}_2\text{O}$ -Met3-Heated	3	4.270474	1.70E-04	3.865
$\text{Cu}_2\text{O}$ -Ser3	3	4.254187	-3.64E-03	2.09
$\text{Cu}_2\text{O}$ -Ser3-Heated	3	4.265471	-1.00E-03	2.878
$\text{Cu}_2\text{O}$ -Lys3	3	4.248949	-4.87E-03	1.126
$\text{Cu}_2\text{O}$ -Lys3-Heated	3	4.270560	1.90E-04	1.956
$\text{Cu}_2\text{O}$ -Asp3	3	4.264375	-1.26E-03	1.718
$\text{Cu}_2\text{O}$ -Asp3-Heated	3	4.269976	5.32E-05	3.682
$\text{Cu}_2\text{O}$ -Pro3	3	4.264633	-1.20E-3	2.105
$\text{Cu}_2\text{O}$ -Pro3-Heated	3	4.270552	1.88E-04	4.786
$\text{Cu}_2\text{O}$ -Ala3	3	4.258659	-2.60E-03	1.962
$\text{Cu}_2\text{O}$ -Ala3-Heated	3	4.269283	-1.09E-04	5.582
$\text{Cu}_2\text{O}$ -Thr3	3	4.261653	-1.90E-03	2.608
$\text{Cu}_2\text{O}$ -Thr3-Heated	3	4.268988	-1.78E-04	3.974
$\text{Cu}_2\text{O}$ -Glu3	3	4.264510	-1.23E-03	1.378
$\text{Cu}_2\text{O}$ -Glu3-Heated	3	4.270010	6.11E-05	2.215
$\text{Cu}_2\text{O}$ -Phe3	3	4.265348	-1.03E-03	1.816
$\text{Cu}_2\text{O}$ -Phe3-Heated	3	4.270401	1.53E-04	8.442

Cu <sub>2</sub> O-Ile3	3	4.263399	-1.49E-03	1.842
Cu <sub>2</sub> O-Ile3-Heated	3	4.270266	1.21E-04	3.681
Cu <sub>2</sub> O-Leu3	3	4.263900	-1.37E-03	1.225
Cu <sub>2</sub> O-Leu3-Heated	3	4.270280	1.24E-04	3.169
Cu <sub>2</sub> O-Val3	3	4.265492	-1.01E-03	1.256
Cu <sub>2</sub> O-Trp3	3			
Cu <sub>2</sub> O-Seleno0.5	3	4.255776	-3.28E-03	1.816
Cu <sub>2</sub> O-Tyr3	3	4.263595	-1.45E-03	4.249

Based on the finding that Cu<sub>2</sub>O/Gln composite crystals exhibit the most prominent lattice distortions as compared to the control, the latter sample has been selected to further investigate the effect of heat treatment on the structure of the crystals by means of the in-situ heating system. The experiment was performed within the temperature range of 50°C-300°C. Figure 2 presents the (111) diffraction peak evolution of pure Cu<sub>2</sub>O crystals and Cu<sub>2</sub>O/Gln composite crystals after a heat treatment. Only a rather slight lattice expansion over the temperature and no considerable peak shift were detected after thermal annealing of the control sample (Figure 2A). In contrast, the revealed relaxation behaviour observed for the Cu<sub>2</sub>O/Gln composite indicated that the lattice distortions were continuously-relaxing due to organics are burnt out during the stepwise increase of the applied temperature. In addition, the lattice relaxation already commenced at 75°C and its highest rate was found between 100°C and 150°C. A full relaxation of distortions was observed above 225°C which signifies a complete decomposition of the intracrystalline organic phase (Figure 2B).

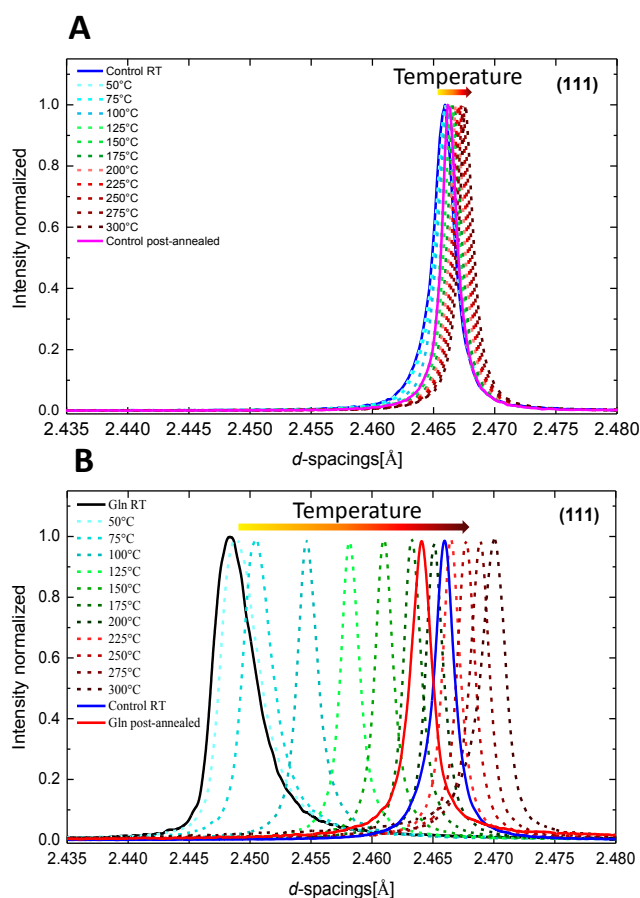


Figure 2: Evolution of (111) reflections for A) Cu<sub>2</sub>O control sample and B) Cu<sub>2</sub>O crystals after incorporation of Gln recorded during different stages of the in-situ heat treatment experiment carried out within temperature range from 50°C (dashed light blue) and up to 300°C (dashed brown) with a step rate of 25°C. In solid: the (111) spectra obtained before and after heat treatment for the control sample (blue and magenta, respectively) and Cu<sub>2</sub>O sample crystallized in the presence of Gln 3mg mL<sup>-1</sup> (black and red, respectively).

With the aim to determine the activation energy of the thermally-activated lattice relaxation we subjected Cu<sub>2</sub>O/Gln crystals to isochronous annealing for 1 hour at 50-300°C temperature range. In difference to the previously performed in-situ annealing where the sample was heated constantly, here the sample was allowed to cool down to room temperature after each heating cycle and prior to recording the diffraction pattern. Temperature-dependent lattice distortions relaxation characterized by the (111) diffraction peak of the Cu<sub>2</sub>O/Gln composite crystals shows a continuous shift towards *d*-spacings values of the control sample (Figure 3a, blue graph – control at ambient temperature, red graph – post annealed Cu<sub>2</sub>O/Gln composite). The lattice distortions along *a,b,c*-axis became practically zero after annealing at 300°C (Figure 3b).

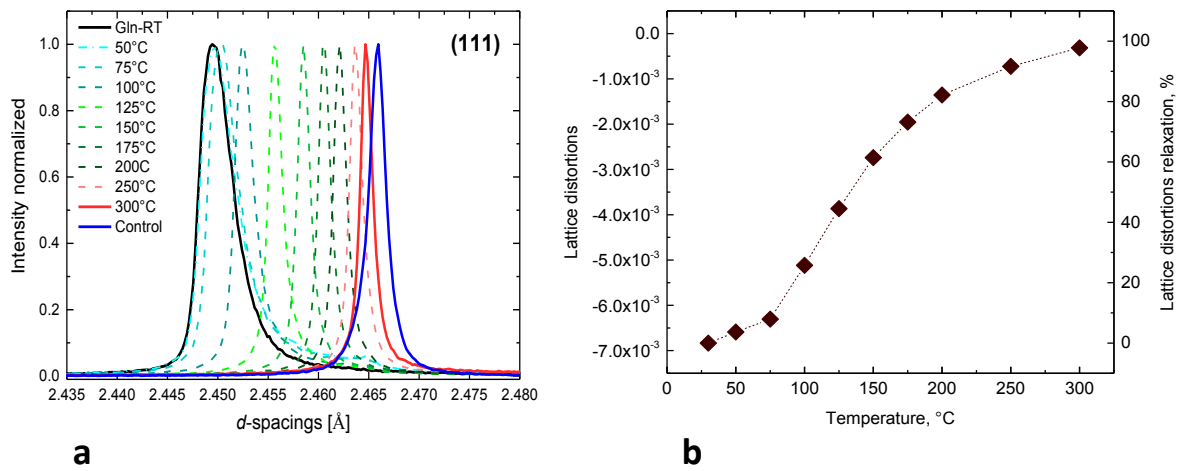


Figure 3. Cu<sub>2</sub>O/Gln composite subjected to the isochronous thermal annealing: a) (111) reflections collected and b) lattice distortions relaxation at every cycle of the annealing process.

The value of activation energy of the temperature-dependent lattice relaxation was derived from our experimental data by employing the Debye relaxation model:  $S(T, t) = S(0) \times \exp(-t/\tau)$ , expressing the relation between lattice distortions before  $S(0)$  and after  $S(T, t)$  annealing at given temperature,  $T$ , for duration,  $t$ . The temperature variation of the relaxation time parameter  $\tau$  is given by an Arrhenius type relation:  $\tau(T) = \tau_0 \exp(\Delta E_a/RT)$ , where  $\tau_0$  represents the relaxation time at infinite temperature (pre-exponential factor),  $\Delta E_a$  the activation energy of the relaxation process,  $R = 8.314 \text{ J mol}^{-1} \text{ K}^{-1}$  is the universal gas constant. The activation energy for lattice relaxation calculated from the slope of a linear fit to these data is about 0.23eV. Considering that the activation energy of protein unfolding is known to be in the range of 0.1 - 1 eV, the obtained reasonably low value we attribute to the thermal decomposition of intracrystalline organic matter occurring under mild heat treatments and leading to the lattice relaxation. Moreover, previous study conducted on biogenic aragonitic shells reports the activation energy of 0.31eV for the temperature-induced lattice relaxation originating from the destruction of the occluded organic macromolecules. The latter reasoning strengthens the idea that the lattice relaxations along the *a,b,c*-axes of the Cu<sub>2</sub>O unit cell observed under mild heat treatments arises exclusively due to the disruption of organic inclusions.

In conclusion, accurate measurements of the structural parameters in bio-inspired semiconductor crystals conducted at ID22 will allow us further to learn how the chemical structure and the length of the incorporated biomolecules affects the semiconductor's crystal structure and band gap. Utilizing the obtained results we do hope to decipher the mechanism of band gap change due to such incorporation. Moreover, for better understanding of the incorporation of biomolecules inside the crystal structure, an accurate concentration measurement of intracrystalline molecules needs to be further performed.